İSTANBUL TİCARET ÜNİVERSİTESİ
FEN BİLİMLERİ DERGİSİ

İstanbul Commerce University Journal of Science

http://dergipark.org.tr/ticaretfbd

Research Article / Araştırma Makalesi

DESIGN OF PASSIVE HARMONIC FILTER FOR THE CLAW-POLE SYNCHRONOUS GENERATORS UNDER NON-LINEAR LOADING*

PENÇE-KUTUPLU SENKRON GENERATÖRLER İÇİN DOĞRUSAL OLMAYAN YÜKLEME ALTINDA PASİF HARMONİK FİLTRE TASARIMI

Yusuf TOPRAK[1] **Oktay KARAKAYA**[2] **Şevket CANTÜRK**[3]

Murat Erhan BALCI[4]

https://doi.org/10.55071/ticaretfbd.1600837

Corresponding Author (Sorumlu Yazar)	*Received (Geliş Tarihi)*	*Revised (Revizyon Tarihi)*	*Accepted (Kabul Tarihi)*
karakaya@balikesir.edu.tr	*13.12.2024*	*21.03.2025*	*25.03.2025*

Abstract

In this study, firstly, the harmonic distortions of terminal voltage and current of a three-phase 1,5 kVA, 150V, 50 Hz, and four poles permanent magnet excited Claw Pole Synchronous Generator (CPSG) supplying a 6-pulse rectifier load are simulated using its 3D Finite Element Model (FEM) in Ansys Maxwell software environment. Then, various low-pass passive filters are designed with a practical approach to reduce the terminal voltage and winding current harmonics in the analysis system. Finally, the terminal voltage and current harmonic distortions, losses, torque oscillations, and efficiency of the modelled CPSG are evaluated when the designed filter is connected to the system. According to the numerical results obtained, the best-performing filter among the designed ones is determined. It is also concluded that with the help of this best-performing filter, the terminal voltage harmonic distortion, losses, torque oscillations, and efficiency of the CPSG are considerably improved.

Keywords: Claw pole synchronous generator, low-pass passive filter, nonlinear load, filter design.

Öz

Bu çalışmada, ilk olarak, 1,5 kVA, 150V, 50 Hz, dört kutuplu, kalıcı mıknatıs ile uyarılmış Pençe Kutuplu Senkron Generatörün (PKSG), 6 darbeli doğrultucu yükü beslerken terminal gerilimi ve akımındaki harmonik bozulmalarının 3 Boyutlu Sonlu Elemanlar Modeli (SEM) kullanılarak Ansys Maxwell yazılım ortamında simülasyonu gerçekleştirilmiştir. Daha sonra, analiz sistemindeki terminal gerilimi ve sargı akımı harmoniklerini azaltmak için pratik bir yaklaşımla çeşitli alçak geçiren pasif filtreler tasarlanmıştır. Son olarak, tasarlanan filtrelerin sisteme bağlanması durumunda, modellenen PKSG'nin terminal gerilimi ve akım harmonik bozulmaları, kayıpları, tork dalgalanması ve verimi değerlendirilmiştir. Elde edilen sayısal sonuçlardan, tasarlanan filtreler arasında en iyi performansa sahip olan belirlenmiştir. Ayrıca, bu en iyi performansa sahip filtre yardımıyla PKSG'nin terminal gerilim harmonik bozulması, kayıpları, tork dalgalanması ve veriminin dikkate değer ölçüde iyileştirildiği sonucuna varılmıştır.

Anahtar Kelimeler: Pençe kutuplu senkron generatör, alçak geçişli pasif filtre, doğrusal olmayan yük, filtre tasarımı.

* *This publication was produced from the graduate Master thesis of Yusuf TOPRAK in the Electrical-Electronics Engineering Program of Balıkesir University, Institute of Scince.*

[1] Balikesir University, Department of Electrical-Electronics Engineering, Balıkesir, Türkiye.
y.toprak@outlook.com.tr.

[2] Balikesir University, Bigadic Vocational School, Balıkesir, Türkiye.
karakaya@balikesir.edu.tr.

[3] Balikesir University, Sindirgi Vocational School, Balıkesir, Türkiye.
scanturk@balikesir.edu.tr.

[4] Balikesir University, Department of Electrical-Electronics Engineering, Balikesir, Türkiye.
mbalci@balikesir.edu.tr.

1. INTRODUCTION

The Claw Pole Synchronous Generator (CPSG), also called as the Lundell-type generator, is a three-phase alternating current (AC) machine with a diode rectifier (Lequesne, 2015). It is popular in internal combustion vehicles (Lequesne, 2015; Omri et al., 2018a; Whaley et al., 2004). In the recent literature, they are also considered for small-scale wind turbines (Artal-Sevil et al., 2018; Phyo & Aung, 2014). According to the excitation method, CPSGs have three types: electrically excited (Whaley et al., 2004), permanent magnet excited (Jurca, 2016), and hybrid excited (excitation with both winding and permanent magnets) (Omri et al., 2018a). The rotor constructions of these three types are given in Figure 1. As seen from this figure, the rotor of the CPSG is fabricated by interlocking two iron pieces with claw-shaped protrusions.

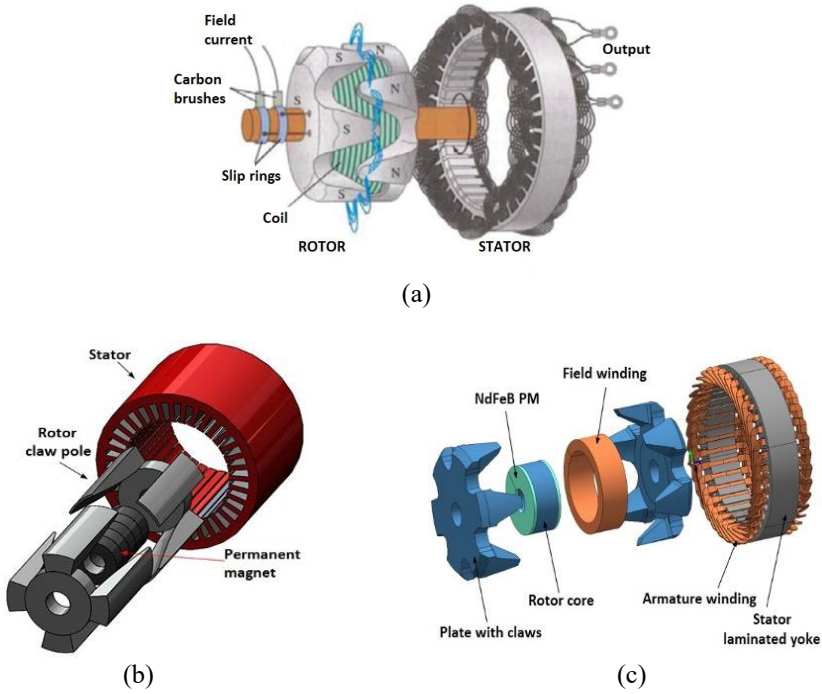

Figure 1. (a) Electrically Excited (Whaley et al., 2004), (b) Permanent Magnet Excited (Jurca, 2016), and (c) Hybrid Excited CPSG (Omri et al., 2018a)

There are several studies in the literature on the performance analysis of CPSGs (Jurca et al., 2006; Jurca et al., 2019; Omri et al., 2018; Pillai et al., 2006; Tan-Kim et al., 2014; Tan-Kim et al., 2017; Wu & Zuo, 2018; Yang et al., 2015; Ye et al., 2018). They are generally conducted with the three-dimensional finite element method (3D FEM) (Jurca et al., 2008; Jurca et al., 2019) and magnetic equivalent circuit (Cao et al., 2022; Ye et al., 2018) based simulations, and measurements (Tan-Kim et al., 2014).

The analysis studies mainly focused on the noise and vibration performances of the machine (Tan-Kim et al., 2014; Tan-Kim et al., 2017; Wu & Zuo, 2018; Yang et al.,

2015). The effects of the design parameters (Wu & Zuo, 2018; Yang et al., 2015), production processes (Tan-Kim et al., 2017), and thermal conditions (Tan-Kim et al., 2014) on the electromagnetic vibration and acoustic noise were investigated. In addition to these studies, Balcı conducted a comparative analysis of the permanent magnet CPSG in terms of efficiency for cores made of various magnetic materials (Balcı, 2024).

Furthermore, some studies aimed to maximize the output torque and efficiency of these machines while minimizing their torque fluctuations, acoustic noise, and losses (Bao & Liu, 2012; Cao et al., 2022; Shuguang et al., 2019; Zhang et al., 2016). Additionally, some works proposed new CPSG designs regarding the geometry and construction material of the rotor (Geng et al., 2020; Hagstedt et al., 2012; Li et al., 2022; Omri et al., 2018a; Zhao et al., 2018).

In another part of the literature on the CPSGs, it was shown in (Jurca et al., 2019) and (Jurca et al., 2008) that the air gap has a significantly distorted waveform of magnetic flux density in the machine. Due to this, they have considerably distorted terminal voltages under no-load and loading conditions (Omri et al. 2018b; Pillai et al., 2006; Ye et al., 2018). In the study (Toprak et al. 2023), the voltage harmonic distortion and losses of the permanent magnet CPSG were analyzed under different loading levels of the uncontrolled six-pulse rectifier load. They also investigated the same performance quantities for various values of the circuit parameters (snubber capacitor and choke inductor) of the same load. It was concluded that both the loading level and circuit parameters considerably affect the performance of the CPSG.

The power electronic circuits draw the distorted currents and result in harmonic distortion of the voltages in the system. Thus, they cause a significant increase in winding losses. The increased winding loss leads to overheating of the windings and reduces the lifespan of electrical machines (Cantürk et al., 2024; Fuchs & Masoum, 2011; Singh, 2009). Harmonic distortion also causes torque vibrations in rotating electrical machinery (Donolo et al., 2016). It is well known in the literature that harmonic filters are employed to avoid the detrimental effects of harmonic distortion on power system equipment. However, according to the best knowledge of the authors, there is no study on the application of harmonic filters to mitigate the harmonic distortion of terminal voltages and currents of the CPSG under nonlinear loading conditions (Toprak, 2023; Toprak et al., 2024).

In this study, firstly, the terminal voltage and winding current harmonic distortions of a three-phase 1,5 kVA, 150 V, 50 Hz, four-pole, permanent magnet (PM) excited CPSG supplying a 6-pulse rectifier are simulated using a three-dimensional (3D) Finite Element (FE) Model in the Ansys Maxwell software environment (ANSYS Innovation Courses, 2020; Rosu et al., 2017). Then, various low-pass passive filters are designed with a practical approach to reduce the terminal voltage and winding current harmonics in the analysis system. Finally, the terminal voltage and current harmonic distortions, losses, torque oscillations, and efficiency of the modelled CPSG are evaluated when the designed filters are connected to the system, and the best-performing filter among the designed ones is determined.

This study is produced from the M.Sc. of the first author (Toprak, 2023), and it is partly presented in the abstract paper for the 3rd International Conference on Applied Mathematics in Engineering (Toprak et al., 2024).

2. HARMONIC ANALYSIS OF THE PM EXCITED CPSG SUPPLYING SIX-PULSE RECTIFIER LOAD

In this section, the 3D FE modelling of the 3-phase 4-pole PM excited CPSG with rated values of 1,5 kVA, 150 V, 1500 rpm and 50 Hz, which is considered for the analyses, is introduced in Ansys Maxwell software environment (ANSYS Innovation Courses, 2020; Rosu et al., 2017). In addition to that, for its analysis under the loading conditions, the equivalent circuit of the considered CPSG is provided using Circuit Editor module of Ansys Maxwell. Lastly, a six-pulse uncontrolled rectifier circuit accompanied by a pure resistor and smoothing capacitor at its DC side is modelled as the load of the CPSG in the Simplorer environment.

2.1. Modelling of the Simulated CPSG in Maxwell 3D

The studied CPSG is a modified version of the model that existed in the library of the Ansys Maxwell. It is modified by using RMxprt module of the Ansys Maxwell. And then, it is transferred to the 3D FEM module of the software. Note that due to the asymmetrical rotor structure of the CPSG, its FE analysis can be achieved with 3D modelling. Detailed views of the 3D model of the studied CPSG are shown in Figure 2 (Toprak et al., 2023; Toprak et al., 2024).

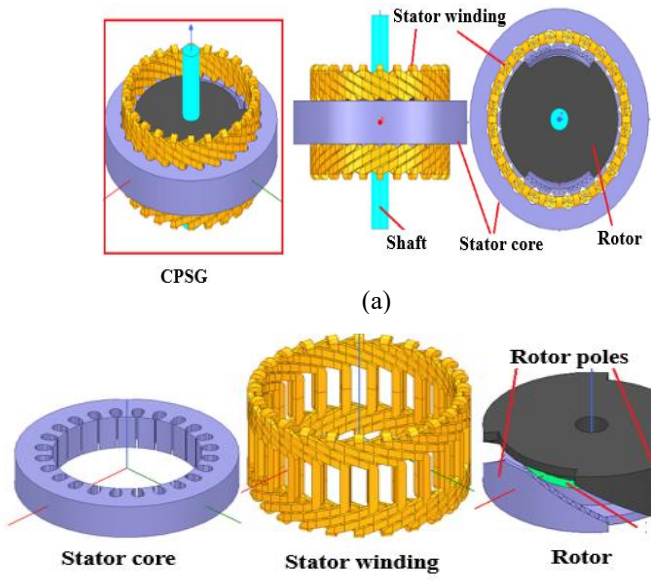

Figure 2. (a) Complete View of the 3D Model From Different Perspectives and (b) Stator Core, Stator Winding, and Rotor Views of the Model Separately.

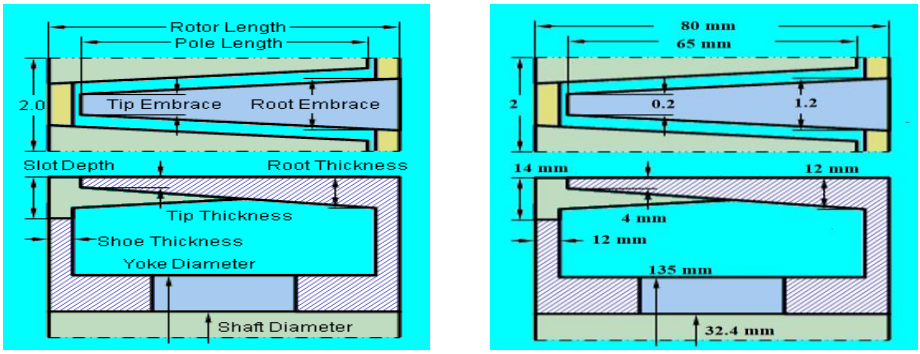

(a) (b)

Figure 3. (a) Rotor Pole Parameters and (b) Their Sizes.

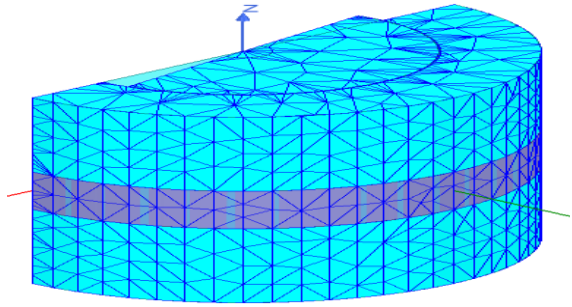

Figure 4. The 3D Mesh View of the Modelled CPSG.

It is seen from Figure 2 that the modelled machine has four poles and PM excitation, and its stator contains 24 slots. The type of PMs, rotor core material, and stator core material are selected as XG196/96, 1008 steel, and JFE Steel 35JN360, respectively. The inner/outer diameters and length of the stator are 216 mm, 324 mm, and 65 mm, respectively. The diameter and length of the rotor are 212,76 mm and 80 mm, respectively. Other rotor pole parameters and their sizes are detailed in Figure 3. The 3D mesh view of the modelled CPSG is given in Figure 4. The number of the mesh elements is automatically set to 90037 by Ansys Maxwell. Here, it should also be noted that to reduce the analysis time, only half of the machine geometry is simulated.

2.2. Creation of the Equivalent Circuit in Maxwell Circuit Editor

For the filter design study, the equivalent circuit of the CPSG modeled in Ansys Maxwell 3D is provided by the Maxwell Circuit Editor environment. The provided equivalent circuit is shown in Figure 5. In this circuit, voltmeters and ammeters are placed to measure the generator's terminal phase voltages, terminal line voltages, and terminal currents. In the circuit given in Figure 5, there is no load. In other words, the generator is operating under no-load conditions. Under no-load conditions, the magnitudes of the terminal voltage harmonic components, per the magnitude of the fundamental harmonic, are presented in Figure 6. In this figure, the blue, green, and red lines represent the harmonic components for the three phases line voltages. It can be

mentioned from the harmonic spectrum that the line voltages have significant harmonic distortion, and their dominant harmonic components are the 7th, 13th, 19th, 21st, and 39th harmonics.

In addition to that, for the analysis, the total harmonic distortion (THD_V) and RMS (V_L) values of the terminal line voltages are calculated using Equation (1) and (2) (Toprak, 2023):

$$THD_V = \frac{\sqrt{\sum_{h\geq 2} V_h^2}}{V_1} 100 \quad (1)$$

$$V_L = \sqrt{\sum_{h\geq 1} V_h^2} \quad (2)$$

where V_1 and V_h denote the fundamental and non-fundamental harmonic voltages.

Accordingly, for the no-load operation of the modelled CPSG, V_L and THD_V are approximately found as 186 V and 14%.

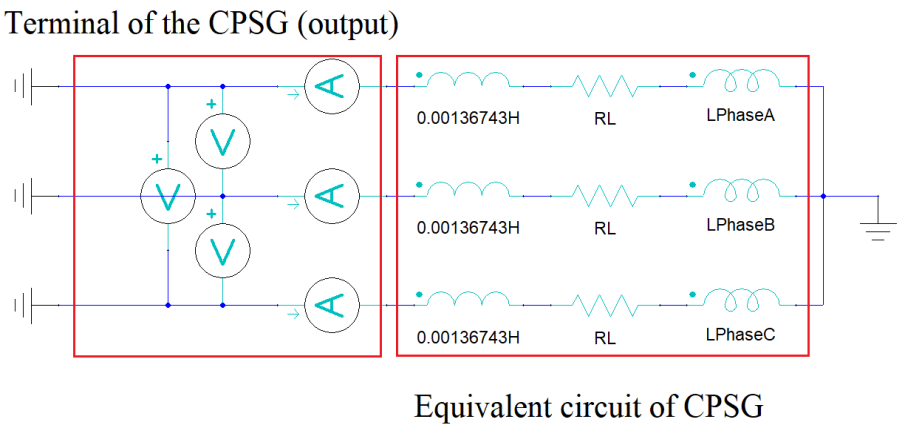

Figure 5. The Equivalent Circuit of the CPSG in Maxwell Circuit Editor Environment.

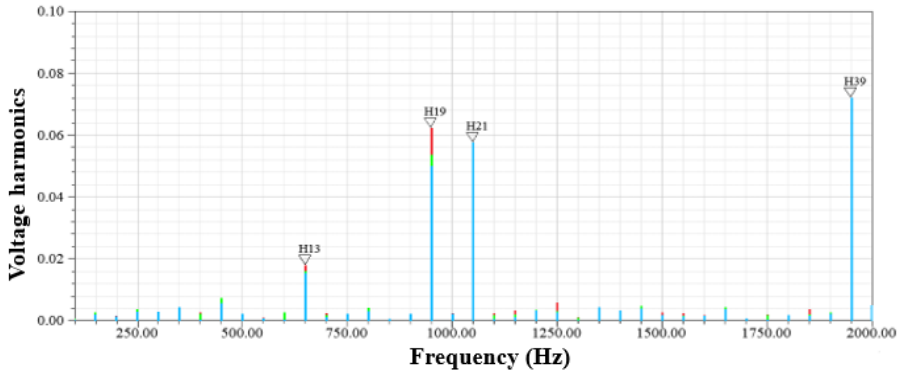

Figure 6. Harmonic Spectrum of the Terminal Line Voltages of the CPSG Under No-Load Condition.

2.3. Modelling of Six-pulse Rectifier Load

For the analysis, a six-pulse uncontrolled rectifier circuit accompanied by a pure resistor and smoothing capacitor at its DC side is considered as a load of the CPSG in this study. Accordingly, the rectifier load is modelled in Ansys Maxwell Circuit Editor. The equivalent circuit model of the CPSG supplying the rectifier load is completely given in Figure 7. In the circuit, R_d and C_d values are selected as 5Ω and 125μF, respectively. For these two-circuit parameter, the loading ratio of the CPSG is nearly 100%, and the relative ripple of the rectifier's DC output voltage is 4,3%.

To evaluate the performance parameters of the CPSG such as harmonic distortion of terminal voltage and current and losses, firstly, the system without the filter is simulated. Due to this, there is no filter in the system shown in Figure 7. The total harmonic distortion (THD_I) of the terminal current is calculated using the non-fundamental (I_h) and fundamental harmonics effective values as follows (Toprak, 2023):

$$THD_I = \frac{\sqrt{\sum_{h\geq 2} I_h^2}}{I_1} 100 \tag{3}$$

In addition to that, by means of the machine loss calculation tools, the core and winding losses are found. In the Ansys Maxwell, for a frequency (f), the total core loss is calculated regarding maximum magnetic flux density (B_{max}), Hysteresis coefficient (K_H), classic eddy current coefficient (K_c), and additional loss coefficient (K_e) (ANSYS Innovation Courses, 2020; Tikhonova et al., 2017).

$$P_C = K_H B_{max}^2 f + K_c B_{max}^2 f^2 + K_e B_{max}^{1,5} f^{1,5} \tag{4}$$

Since the rotor is excited by the permanent magnets, the winding losses consist of only stator winding losses (P_W) for the modelled CPSG. P_W can be found using current density (J) and electrical conductivity of windings (Tikhonova et al., 2017):

$$P_W = \frac{1}{\sigma}\iiint J^2 dV \tag{5}$$

Accordingly, the sum of P_W and P_C gives the total loss (P_T) of the CPSG:

$$P_T = P_C + P_W \tag{6}$$

By neglecting the windage and frictional losses, the efficiency of the CPSG is approximately computed as the ratio of output power and input power:

$$\eta(\%) = 100\frac{P}{P_T+P} \tag{7}$$

Where P is the active power at the terminal, and it is calculated by averaging of sum of the instantaneous powers drawn from a, b and c phases for a period (T) (Balci, 2009):

$$P = \frac{1}{T}\int_0^T (v_a i_a + v_b i_b + v_c i_c)dt \tag{8}$$

Last performance parameter is the relative value of the torque oscillation that is calculated as follows:

$$\Delta T = 100\frac{(T_{max} - T_{min})}{T_{av}} \tag{9}$$

Where T_{max}, T_{min}, and T_{av} stand for maximum, minimum, and average values of the shaft torque, and all are calculated by using Ansys Maxwell tool.

Thus, for the modelled six-pulse rectifier without a passive filter, the V_L and THD_V of the terminal line voltages and the THD_I values of the line currents drawn by the rectifier are given in Table 1. It can be mentioned from this table that the average values of the respected quantities are 131,46 V, 27,86%, and 4,99%. Thus, one can see that THD_V and THD_I have considerable values that may lead to an increase in both core and winding losses, and overheating in the machine. Note that for the same case, the losses (P_C, P_W, P_T) and the torque oscillation (ΔT) values of the CPSG are calculated as 21,73 W, 78,40 W, 100,13 W, and 21,23%, respectively.

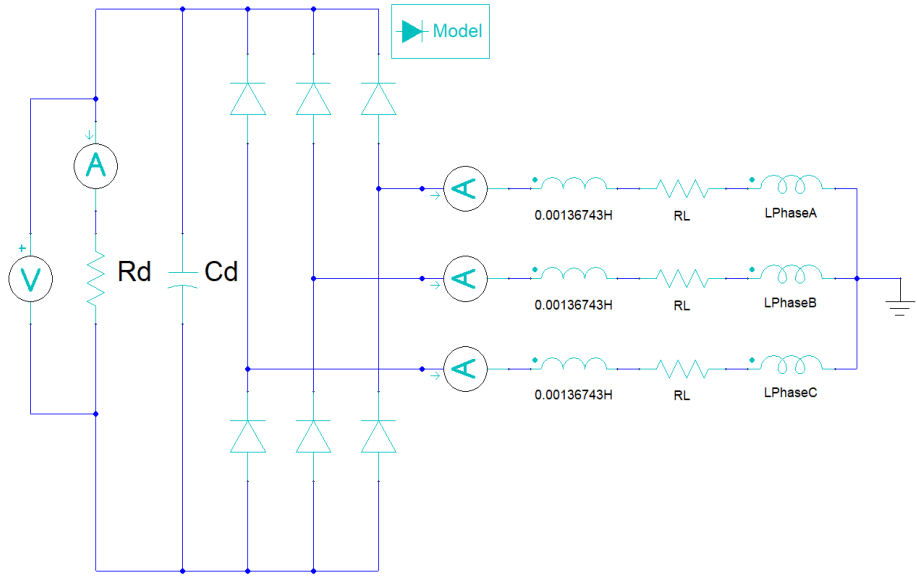

Figure 7. The Equivalent Circuit Model of the CPSG Supplying the Rectifier Load in Ansys Maxwell Circuit Editor Environment.

Table 1. V_L, THD_V, and THD_I Values at the Terminal of CPSG Supplying the Six-Pulse Rectifier Without a Passive Filter.

	V_L (V)	**THD_V (%)**	**THD_I (%)**
L1	130,92	29,02	4,58
L2	130,90	27,60	5,93
L3	132,56	26,97	4,45
Average	131,46	27,86	4,99

3. DESIGN OF PASSIVE HARMONIC FILTER

In this section, to mitigate harmonic distortion of the terminal voltage and current, and reduce the losses and the torque oscillation of the CPSG under nonlinear loading, it is aimed to design a passive filter.

For the harmonic mitigation in the electric power networks, several tuned passive filter types are employed in the literature (Fuchs, 2011; Karadeniz & Balci, 2018). However, in this study, to effectively filter a large number of harmonic components in a wide frequency range in the terminal voltage and current, the low-pass LC filter is preferred instead of tuned filters. The single-phase circuit of the low-pass filter is given in Figure 8.

The resonance frequency of the filter can be written in terms of L_f and C_f as follows (Adak, 2021; Zubi, 2005c).

$$f_r = \frac{1}{2\pi\sqrt{L_f C_f}} \tag{10}$$

The delta-connected three-phase filter, which is illustrated in Figure 9, is employed in the analysis system. Therefore, regarding Equation 11, the resonance frequency of the delta connected filter can be written:

$$f_r = \frac{1}{2\pi\sqrt{L_f 3C_{f\Delta}}} \tag{11}$$

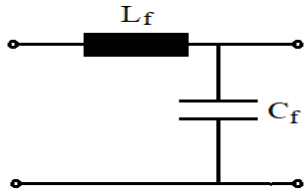

Figure 8. The Single-Phase Circuit of the Low-Pass Filter.

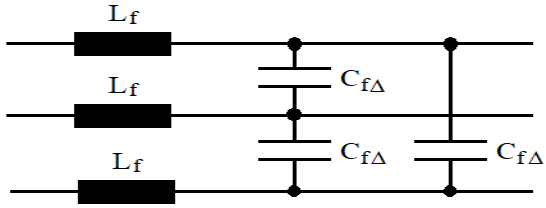

Figure 9. The Delta-Connected Three-Phase Circuit of the Low-Pass Filter.

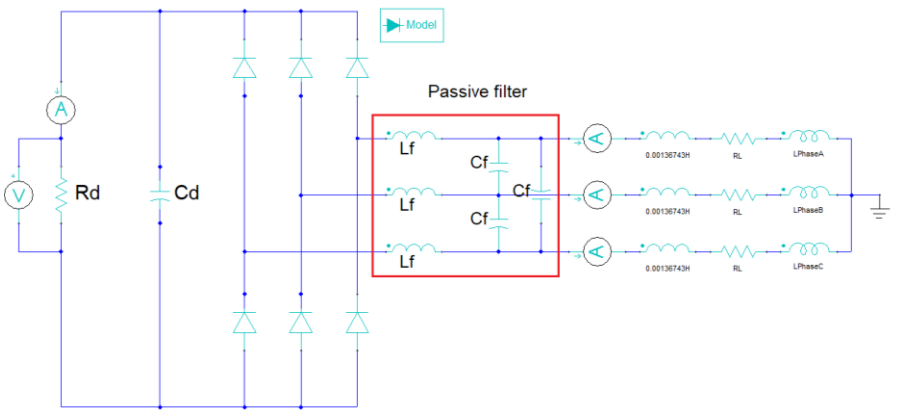

Figure 10. The Circuit of the System With The Low-Pass Passive Filter Provided in Ansys Maxwell Circuit Editor.

The circuit of the system with the low-pass passive filter provided in Ansys Maxwell Circuit Editor is given in Figure 10.

Since the performance parameters of the CPSG is obtained by 3D FE analysis, optimization of the filter parameters is a highly time-consuming process. Due to this, in this study, the proper values of the filter parameters are practically achieved by generating possible solutions in the feasible region. The considered approach has three stages:

- First stage: Analyse the effect of the filter inductor (L_f) on the performance parameters of the CPSG, and choose a feasible value for the inductor accordingly. In this step, only the inductors of the filter exist in the circuit, while its capacitors are disconnected from the circuit.
- Second stage: Determine resonance frequency (f_r) according to the lowest harmonic order in the system and find the filter's capacitor ($C_{f\Delta}$) using Eq. 11.
- Last stage: Test the system with the filter, and evaluate the losses, loading level, torque oscillation, terminal voltage distortion, and terminal current distortion of the CPSG.

3.1. Determination of the Filter's Inductance (Lf)

Here, it is aimed to determine the feasible value of the filter's inductor. To achieve this, the effect of the inductor on the performance parameters of the CPSG is evaluated. Accordingly, for the filter's inductance values (L_f) as 2,5 mH, 5 mH, and 10 mH, the system is simulated. The results are given in Figure 11 and Figure 12.

It is observed from Figure 11 that the average V_L levels for L_f values as 2,5 mH, 5 mH, and 10 mH are 128,63 V, 123,83 V, and 120,71 V, respectively. Thus, it can be mentioned that the effective value of terminal voltages decreases as L_f increases. The same figure also shows that for L_f values of 2,5 mH, 5 mH, and 10 mH, P_T is 93,16, 88,15, and 77,77 W, respectively. For the same inductance values, P_C is 20,89, 20,34, and 19,32 W, while P_W is 72,27, 67,81, and 58,45 W, respectively. As a result, losses decrease with the increment of L_f. In addition to these results, Figure 12 indicates that the average values of THD_I and THD_V are 4,82% and 28,68% for L_f=2,5 mH, 4,55% and 24,34% for L_f=5 mH, and 4,37% and 21,66% for L_f=10 mH. Therefore, one can see that an increase in L_f value improves THD_V and THD_I. Lastly, it can be concluded from the analysis that the tested two L_f values 5 mH and 10 mH cause considerable reduction in THD_V and THD_I. Due to this case, in the second stage, they will be considered for the filter design.

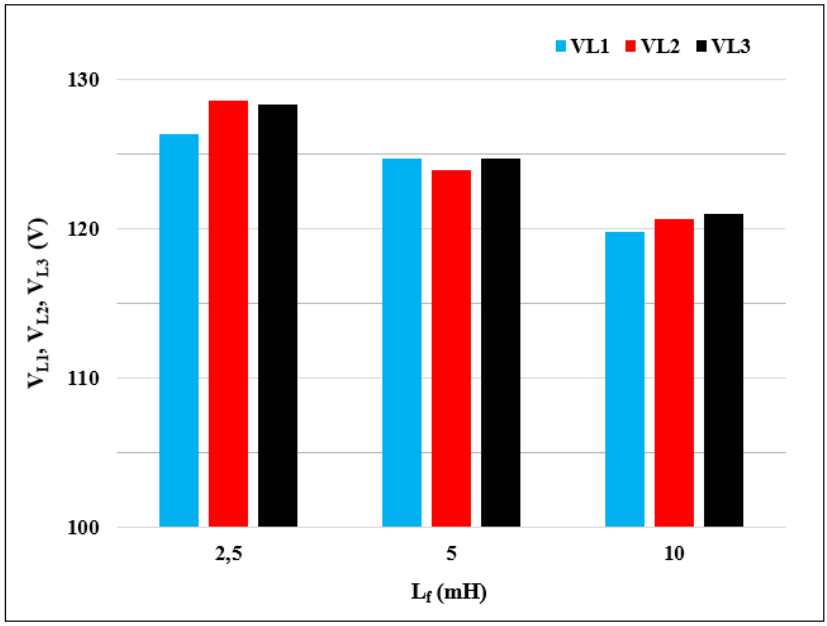

(a)

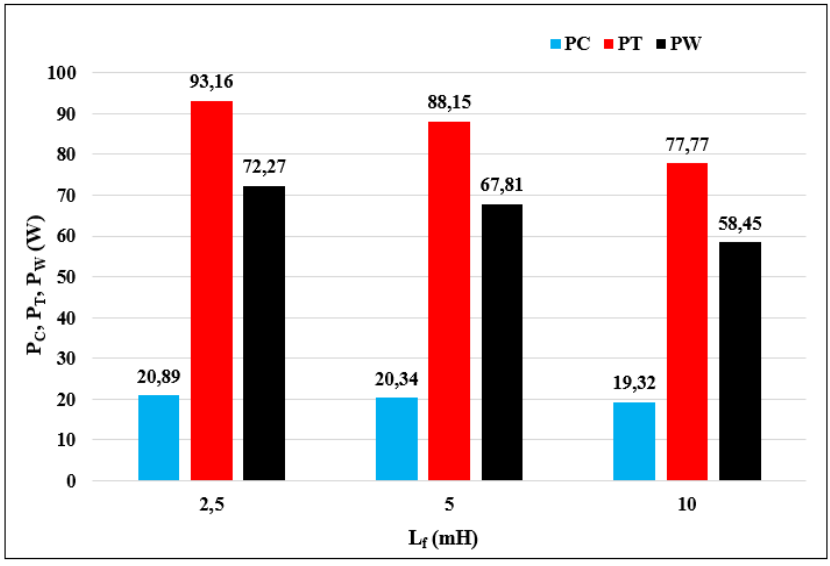

(b)

Figure 11. (a) The RMS Terminal Voltages and (b) Losses of the CPSG For Three L_f Values.

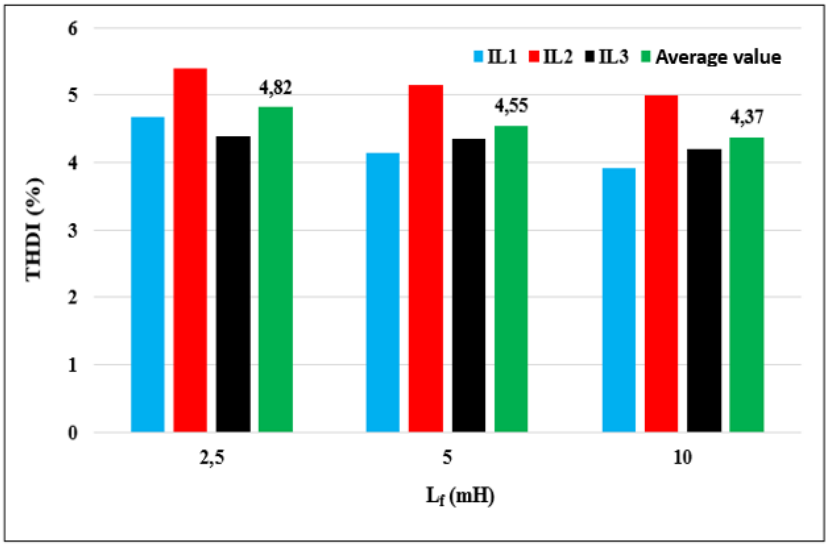

(a)

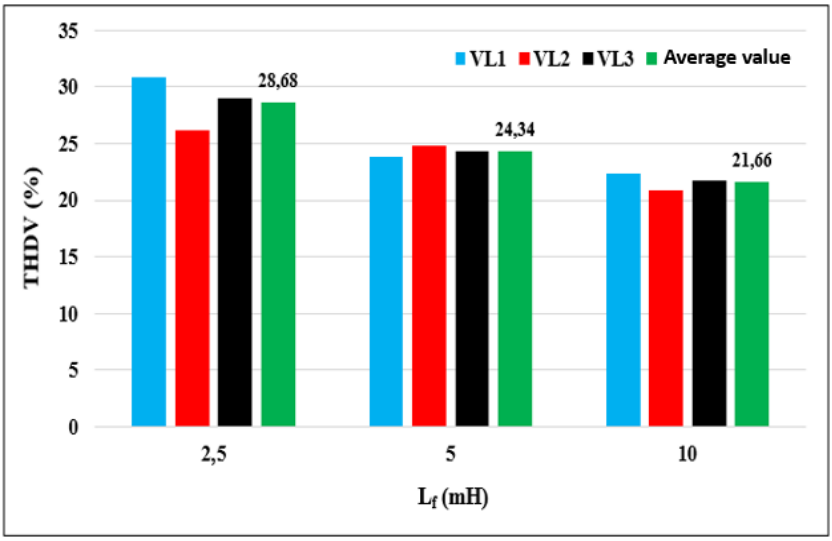

(b)

Figure 12. (a) THD_V and (b) THD_I Values for Three L_f Values.

3.2. Determination of the Resonance Frequency (f_r) and Filter's Capacitors ($C_{f\Delta}$)

It is seen from Figure 6 that the lowest order harmonic of the no-load terminal voltages of the CPSG is the 3rd one. In addition to that, it is well-known from the literature that six-pulse rectifiers draw currents that contain odd-numbered, non-triplen harmonics such as the 5th, 7th, 11th, etc. Accordingly, to reduce the harmonic distortion of terminal voltage and current, the resonance frequency of the filter (f_r) is set to 145 Hz (slightly below the 3rd harmonic) and 205 Hz (below the 5th harmonic).

Regarding two filter inductor values (5 mH and 10 mH) and two resonance frequency values (145 Hz and 205 Hz), four filter choices can be provided as in Table 2.

In the last stage, the performance parameters of the CPSG supplying the six-pulse rectifier will be evaluated for these four filter designs, and the best one will be selected.

Table 2. The Parameters of Determined Four Filter Designs.

	L_f	$C_{f\Delta}$	f_r
Design 1	5mH	81μF	145 Hz
Design 2		41,2μF	205 Hz
Design 3	10 mH	40,5μF	145 Hz
Design 4		20,6μF	205 Hz

3.3. Evaluation of the Performance Parameters of the CPSG for the Designed Filters

The performance parameters of the CPSG supplying six-pulse rectifier load compensated with the determined four filter designs are presented in Table 3.

Table 3. Obtained Results for the Determined Four Filter Designs.

	Design-1	**Design-2**	**Design-3**	**Design-4**	**No filter**
P (W)	2283,42	1774,23	1505,72	1305,62	1531
V_L (V)	152,56	135,52	137,44	126,98	131,46
THD_V (%)	7,44	15,24	9,46	22,53	27,86
THD_I (%)	3,62	4,30	4,12	5,22	4,99
P_T (W)	157,55	116,08	85,94	82,83	100,13
ΔT(%)	12,63	17,09	11,09	25,79	21,23
Efficiency-η (%)	93,54	93,85	94,60	94,03	93,87

This table shows that designs 1 and 3 significantly reduce THD_V and THD_I values. THD_V and THD_I values are 7,44% and 3,62% for design 1, and 9,46% and 4,12% for design 3. Among these two designs, design 1 results in overloading, and it provides lower efficiency (η) in CPSG when compared to the other one.

Besides, for the six-pulse rectifier load compensated with the design 3 filter, the P, V_L, THD_V, THD_I, P_T, ΔT and η of the CPSG are 1505,72 W, 137,44 V, 9,46%, 4,12%, 85,94 W, 11,09 and 94,60%. Therefore, it can be mentioned that design 3 filter can properly be used for harmonic mitigation of the CPSG supplying the six-pulse rectifier under its rated loadig level.

For the system with design 3 filter, the magnitudes of the voltage and current harmonics at the terminal in terms of fundamental ones are plotted in Figure 13.

This figure clearly shows that the filter does not cause any resonance problem in the system.

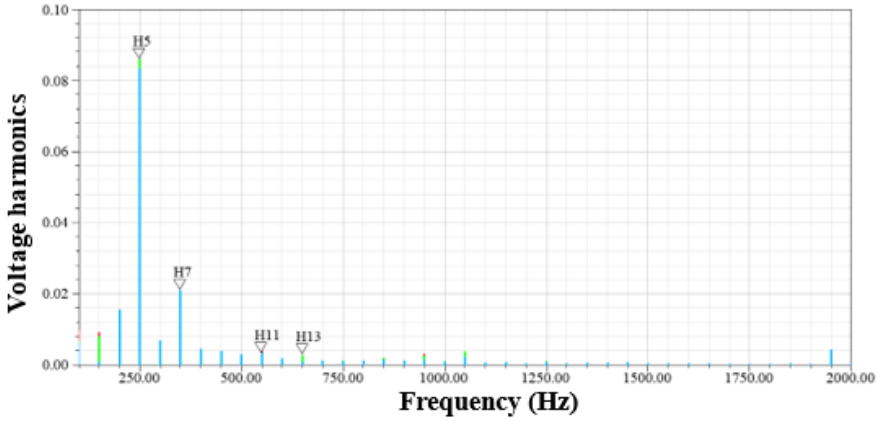

(a)

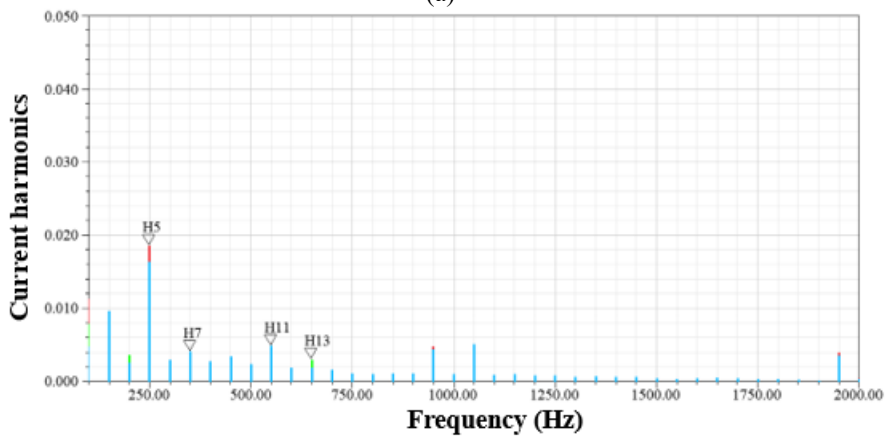

(b)

Figure 13. The Magnitudes of Voltage and Current Harmonics at the Terminal in Terms of Fundamental Ones for the System With Design 3 Filter.

4. CONCLUSION

The harmonic currents and voltages have detrimental effects on the rotational electric machines such as increased losses, overheating, and torque oscillations. Due to these effects, they may have reduced life span. To prevent the reduction in the life span of the rotational machines operated in the distorted systems, the harmonic filters can be employed.

In internal combustion vehicles, claw pole synchronous generators (CPSGs) are employed to supply the electric loads and charge batteries. The ac energy at the terminals of the CPSGs is converted to the DC energy by means of the rectifiers. Thus, these generators are operated under highly distorted load currents. In addition to that, due to the geometry of their rotors, their no-load voltages have considerable harmonic distortion.

In this study, which was partly presented ICAME'24 conference (Toprak et al., 2024), it is aimed to design a passive harmonic filter for the harmonic mitigation of the permanent magnet CPSGs devoted to supplying the six-pulse rectifier loads. For this aim, firstly, the 3D FEM model of a CPSG is provided in Ansys Maxwell environment. Secondly, using Ansys Maxwell circuit editor, a six-pulse rectifier circuit is modelled as a load of the CPSG. And then, in a practical way, several low-pass passive filters are designed to reduce the harmonic pollution of the terminal voltages and currents in the analysis system consisting of the CPSG and six-pulse rectifier load. Finally, the designed filters are tested, and the best one is determined by evaluating the efficiency (η), total losses (PT), relative torque oscillation (ΔT), terminal voltage total harmonic distortion (THD_V), and terminal current total harmonic distortion (THD_I) of the studied CPSG. As a result, it is concluded that low-pass filters can properly be used to avoid the negative effects of the harmonic distortion on the CPSG.

This study investigated the performance of the CPSG for a six-pulse uncontrolled rectifier load. Additionally, only a low-pass filter was used to mitigate the harmonic distortion in the terminal voltage and current. Due to the 3D analysis of the CPSG, systematic optimization would require a significant amount of time. Thus, a systematic algorithm was not employed to design the passive filter in this study.

In future studies, the authors plan to perform a comparative performance analysis of the low-pass harmonic filter with other filter types for several nonlinear loading conditions of CPSGs. They will also try to propose a computationally efficient method for optimization of the filter within Ansys Maxwell environment.

Authors' Contributions
In this study, the first and second authors conducted the modelling and simulation of the system, all authors contributed to writing of the article and analysing of the results, and the fourth author defined and directed the study's focus.

Conflict of Interest Statement
There is no conflict of interest among the authors.

Statement of Research and Publication Ethics
Research and publication ethics were followed in the study.

REFERENCES

Adak, S. (2021). Harmonics mitigation of stand-alone photovoltaic system using LC passive filter. Journal of Electrical Engineering & Technology, 16(5), 2389-2396.

ANSYS. (2020). Ansys Maxwell Getting Started Module 1: Basics. ANSYS Innovation Courses. Retrieved July 10, 2021, from https://www.courses.ansys.com/wpcontent/uploads/2021/07/MAXW_GS_2020R2_EN_LE01.pdf.

Artal-Sevil, J. S., Dufo, R., Astaneh, M., Domínguez, J. A., & Bernal-Agustín, J. L. (2018). Development of a small wind turbine for stand-alone system in rural environment. Reuse and recycling of electric motors. Renewable Energy and Power Quality Journal (RE&PQJ), 1(16), 745-750.

Balcı, S. (2024). Pençe-Kutuplu Senkron Generatörlerde Yeni Nesil Çekirdek Malzemelerin Kullanımıyla Performans Artışı. Muş Alparslan Üniversitesi Mühendislik Mimarlık Fakültesi Dergisi, *5*(2), 20-38.

Balci, M. E., & Hocaoglu, M. H. (2009, November). Comparative review of multi-phase apparent power definitions. In *2009 International Conference on Electrical and Electronics Engineering-ELECO 2009*, I-144. IEEE.

Bao, X. H., & Liu, M. Z. (2012). Parameter analysis and optimal design for mobile Claw-pole alternator. Applied Mechanics and Materials, 130, 658-661.

Cao, Y., Zhu, S., Yu, J., & Liu, C. (2022). Optimization design and performance evaluation of a hybrid excitation claw pole machine. Processes, 10(3), 541.

Cantürk, Ş., Karakaya, O., Balci, M. E., & Aleem, S. H. A. (2024). Introductory chapter: effects of power quality problems on energy efficiency of power systems. Energy Efficiency of Modern Power and Energy Systems (pp. 1-17). Elsevier.

Donolo, P., Bossio, G., De Angelo, C., García, G., & Donolo, M. (2016). Voltage unbalance and harmonic distortion effects on induction motor power, torque and vibrations. Electric power systems research, 140, 866-873.

Fuchs, E. F., & Masoum, M. A. (2011). Power quality in power systems and electrical machines. Academic press.

Geng, H., Zhang, X., Zhang, Y., Hu, W., Lei, Y., Xu, X., ... & Shi, L. (2020). Development of brushless claw Pole electrical excitation and combined permanent magnet hybrid excitation generator for vehicles. Energies, 13(18), 4723.

Hagstedt, D., Reinap, A., Ottosson, J., & Alaküla, M. (2012, September). Design and experimental evaluation of a compact hybrid excitation claw-pole rotor. *In 2012 XXth International Conference on Electrical Machines*. (pp. 2896-2901).

Jurca, F. N. (2016, July). Design of a low-cost permanent synchronous machine for isolated wind conversion systems. In Wind Turbines-Des., Control and Appl. 95-120. IntechOpen.

Jurca, F., Martis, C., & Biro, K. (2009, June). Comparative analysis of the claw-pole rotor dimensions influence on the performances of a claw-pole generator for wind applications. *In 2009 International Conference on Clean Electrical Power*. (pp. 715-720).

Jurca, F., Martis, C., Birou, I., & Biro, K. (2008, May). Analysis of permanent magnet claw-pole synchronous machine. *In 2008 11th International Conference on Optimization of Electrical and Electronic Equipment*. (pp. 75-80).

Karadeniz, A., & Balci, M. E. (2018). Comparative evaluation of common passive filter types regarding maximization of transformer's loading capability under non-sinusoidal conditions. Electric Power Systems Research, 158, 324-334.

Lequesne, B. (2015). Automotive electrification: The nonhybrid story. IEEE Transactions on Transportation Electrification, 1(1), 40-53.

Li, B., Li, X., Wang, S., Liu, R., Wang, Y., & Lin, Z. (2022). Analysis and cogging torque minimization of a novel flux reversal claw pole machine with soft magnetic composite cores. Energies, 15(4), 1285.

Omri, R., Ibala, A., & Masmoudi, A. (2018, April). 3D-FEA based-comparison of different topologies of claw-pole alternators with a dual excitation. *In 2018 Thirteenth International Conference on Ecological Vehicles and Renewable Energies (EVER)*. 1-6.

Omri, R., Ibala, A., & Masmoudi, A. (2018, April). Characterization on the no-and on-load operations of an improved claw pole machine. *In 2018 Thirteenth International Conference on Ecological Vehicles and Renewable Energies (EVER)*. (pp. 1-8).

Phyo, S. P., & Aung, T. H. (2014). Wind turbine generation system implemented with a claw pole alternator. International Journal of Scientific Engineering and Technology Research, 3(16), 3411-3416.

Pillai, K. P. P., Idiculla, M. K., & Nair, A. S. (2006). Spectral study on the voltage waveform of claw pole automotive alternator. European Council for Modeling and Simulation, 456-461.

Rosu, M., Zhou, P., Lin, D., Ionel, D. M., Popescu, M., Blaabjerg, F., ... & Staton, D. (2017). Multiphysics simulation by design for electrical machines, power electronics and drives. John Wiley & Sons.

Shuguang, Z., Xiaorui, H., Yaodan, Z., & Shuanglong, W. (2019). Rotor shape optimization of claw-pole alternator to reduce acoustic noise caused by electromagnetic forces. IEEE Transactions on Energy Conversion, 34(4), 2118-2125.

Singh, G. K. (2009). Power system harmonics research: a survey. European Transactions on Electrical Power, 19(2), 151-172.

Tan-Kim, A., Hagen, N., Lanfranchi, V., Clénet, S., Coorevits, T., Mipo, J. C., ... & Palleschi, F. (2017). Influence of the manufacturing process of a claw-pole alternator on its stator shape and acoustic noise. IEEE Transactions on Industry Applications, 53(5), 4389-4395.

Tan-Kim, A., Lanfranchi, V., Legranger, J., Palleschi, F., & Redon, M. (2014, September). Influence of temperature on the vibro-acoustic behavior of claw-pole alternators. *In 2014 International Conference on Electrical Machines (ICEM)*. (pp. 1628-1634).

Tikhonova, O., Malygin, I., Beraya, R., Sokolov, N., & Plastun, A. (2017). Loss calculation of induction motor with ring windings by "ANSYS Maxwell". APEET, 2017, 63-66.

Toprak, Y., Karakaya, O., Cantürk, Ş., & Balcı, M. E. (2023, December). Analysis on Performance of Claw Pole Synchronous Generators for 6-Pulse Rectifier Load. *4th International Turkish World Engineering and Science Congress*, (pp. 361–371).

Toprak, Y. (2023). *Performance analysis of claw pole synchronous generator under non-linear loading conditions* [Master's thesis]. Balikesir University.

Toprak, Y., Karakaya, O., Canturk, S., & Balci, M. E. (2024, July). Design of Passive Harmonic Filter for the Claw-Pole Synchronous Generators under Non-linear Loading. *The Third International Conference on Applied Mathematics in Engineering* (*ICAMΣ'24)*. (pp. 113).

Whaley, D. M., Soong, W. L., & Ertugrul, N. (2004, September). Extracting more power from the Lundell car alternator. *In Australasian Universities Power Engineering Conference (AUPEC 2004)*. 26-29.

Wu, S., & Zuo, S. (2018). Characteristics analysis of electromagnetic force and noise of claw pole alternators with different pole and slot combinations and phase number. IET Electric Power Applications, 12(9), 1357-1364.

Yang, F., Bao, X., Di, C., & Chen, Z. (2015, October). Simulation and experiment on reducing electromagnetic vibration and noise of claw-pole alternators. *In 2015 18th International Conference on Electrical Machines and Systems (ICEMS)*. (pp. 1452-1458).

Ye, C., Liang, X., Xiong, F., Yang, J., Xu, W., & Liu, Y. (2018). Design of an axial-flux PM-assisted claw-pole generator based on an equivalent magnetic circuit model. IEEE Transactions on Energy Conversion, 33(4), 2040-2049.

Zhang, Z., Liu, H., & Song, T. (2016). Optimization design and performance analysis of a PM brushless rotor claw pole motor with FEM. Machines, 4(3), 15.

Zhao, X., Niu, S., & Ching, T. W. (2018). Design and analysis of a new brushless electrically excited claw-pole generator for hybrid electric vehicle. IEEE Transactions on Magnetics, 54(11), 1-5.

Zubi, H. (2005). *Lowpass broadband harmonic filter design* [Master's thesis]. Middle East Technical University.